

Original Research

Satellite III (1q12) Copy Number Variation in Cultured Human Skin Fibroblasts from Schizophrenic Patients and Healthy Controls

Elizaveta S. Ershova¹, Ekaterina A. Savinova¹, Larisa V. Kameneva¹,
Lev N. Porokhovnik^{1,*}, Roman V. Veiko¹, Tatiana A. Salimova¹, Vera L. Izhevskaya¹,
Sergei I. Kutsev¹, Natalia N. Veiko¹, Svetlana V. Kostyuk¹

¹Laboratory of Molecular Biology, Research Centre for Medical Genetics (RCMG), 115478 Moscow, Russia

*Correspondence: med-gen@mail.ru (Lev N. Porokhovnik)

Academic Editor: Ilaria Baglivo

Submitted: 19 April 2023 Revised: 24 June 2023 Accepted: 14 August 2023 Published: 31 August 2023

Abstract

Background: The chromosome 1q12 region harbors the genome's largest pericentromeric heterochromatin domain that includes tandemly repeated satellite III DNA [SatIII (1)]. Increased SatIII (1) copy numbers have been found in cultured human skin fibroblasts (HSFs) during replicative senescence. The aim of this study was to analyze the variation in SatIII (1) abundance in cultured HSFs at early passages depending on the levels of endogenous and exogenous stress. **Methods:** We studied 10 HSF cell lines with either high (HSFs from schizophrenic cases, $n = 5$) or low (HSFs from healthy controls, $n = 5$) levels of oxidative stress. The levels of endogenous stress were estimated by the amounts of reactive oxygen species, DNA damage markers (8-hydroxy-2'-deoxyguanosine, gamma-H2A histone family member X), pro- and antioxidant proteins (NADPH oxidase 4, superoxide dismutase 1, nuclear factor erythroid 2-related factor 2), and proteins that regulate apoptosis and autophagy (B-cell lymphoma 2 [Bcl-2], Bcl-2-associated X protein, light chain 3). SatIII (1) copy numbers were measured using the nonradioactive quantitative hybridization technique. For comparison, the contents of telomeric and ribosomal RNA gene repeats were determined. RNASATIII (1 and 9) were quantified using quantitative Polymerase Chain Reaction (PCR). **Results:** Increased SatIII (1) contents in DNA from confluent HSFs were positively correlated with increased oxidative stress. Confluent cell cultivation without medium replacement and heat shock induced a decrease of SatIII (1) in DNA in parallel with a decrease in RNASATIII (1) and an increase in RNASATIII (9). **Conclusions:** During HSF cultivation, cells with increased SatIII (1) content accumulated in the cell pool under conditions of exaggerated oxidative stress. This fraction of cells decreased after the additional impact of exogenous stress. The process seems to be oscillatory.

Keywords: schizophrenia; NADPH oxidase 4; nuclear factor erythroid 2-related factor 2; superoxide dismutase 1; gamma-H2A histone family member X; satellite III; copy number variation; human skin fibroblasts

1. Introduction

Tandemly repeated satellite III DNAs (SatIII) are located in regions of pericentromeric heterochromatin. Chromosome-specific subfamilies of SatIII have been identified [1–4], which include SatIII (1) on chromosome 1 (1q12) and SatIII (9) on chromosome 9 (9q12). The SatIII arrays formed on the corresponding chromosomes are the biggest heterochromatin sites in the human genome [5].

Accumulating evidence suggests that satellite repeats play an important role in the formation and maintenance of pericentromeric heterochromatin. Studies have focused on the process of SatIII (9) transcription resulting in the formation of long noncoding RNAs, which are essential for fundamental processes such as development, imprinting, and cell differentiation [6–13]. RNASATIII are also involved in stress responses to heat, hypoxia, and DNA damage [14–30]. SatIII (9) transcription is regulated by heat shock transcription factor 1, which involves RNA polymerase II and depends on the degrees of heterochromatin methylation and decondensation. Activation of the heat shock re-

sponse correlates with the rapid relocalization of HSF1 into nuclear structures termed nuclear stress granules. These stress-induced structures form primarily on the 9q12 region through direct binding of heat shock transcription factor 1 to SatIII [31–33].

SatIII (1) transcription from the 1q12 region in various conditions has been much less studied than SatIII (9) transcription. At the same time, the 1q12 chromosomal region harbors the human genome's biggest site of heterochromatin, which consists of SatII and SatIII tandem arrays. Erukashvily *et al.* [34] were the first to show that SatIII (1) is decondensed, demethylated, and transcribed in senescent cells and A431 epithelial carcinoma cells, in contrast to SatIII (9). It has been also shown that the ratio of the SatIII (1)/SatIII (9) transcript in radiation-exposed cells depends on the ionized radiation (IR) dose [35].

Unlike the SatIII transcription process, copy number variation (CNV) of SatIII repeats in human genomes under various conditions has been poorly studied. Changes in satellite repeat copy numbers are often found in cancer cells



Table 1. Demographic and clinical description of schizophrenic (SZ) patients and healthy controls (K).

#	Index	SZ1	SZ2	SZ3	SZ4	SZ5	K1	K2	K3	K4	K5
1	Age	28	39	42	50	25	35	42	49	39	27
2	Sex	m	m	m	m	m	f	f	m	m	f
3	Age of SZ onset	14	16	17	18	12	n/a	n/a	n/a	n/a	n/a
4	Age of SZ manifestation	15	16	19	19	12	n/a	n/a	n/a	n/a	n/a
5	Relatives with SZ	+	–	+	+	+	–	–	–	–	–
6	Taking antipsychotics	+	+	+	+	+	n/a	n/a	n/a	n/a	n/a

F, Female; M, Male; n/a, Not applicable; #, line number; +, yes; –, no.

[36,37]. Bersani *et al.* [38] presumed that the transcription of satellite DNAs induced by different environmental stress conditions could be coupled to new satellite repeat insertions and changes in the repeat copy numbers. Based on the example of SatII CNV in cancer cells, the mobile nature of satellite DNAs has been suggested [38].

We previously observed changes in SatIII (1) CNVs in mesenchymal stem cells exposed to radiation [35], cultured human skin fibroblasts (HSFs) during replicative senescence and oxidative stress [39], and blood cells from schizophrenic (SZ) patients during antipsychotic treatment [40]. The HSF pool at early passages is heterogeneous with respect to SatIII (1) quantity in cell genomes. Cells with high SatIII (1) content have low proliferative capacity and produce small clones during division. The fraction of these cells increases during replicative senescence [39]. Cells with high SatIII (1) content do not respond to proliferative stimuli and die when exposed to such impacts as inducing an adaptive response in normal cells with low SatIII (1) content. The increase in SatIII (1) content, as observed during the course of senescence, is positively correlated with telomere shortening [39].

The aim of this study was to analyze SatIII (1) CNVs in cultured HSFs at early passages. First, we determined if and how the changes in SatIII (1) content during HSF cultivation at early passages depend on the levels of endogenous oxidative stress in the cell pool. The level of oxidative stress can be assessed by a reactive oxygen species (ROS) assay, by the amount of DNA damage markers (8-oxo-2'-deoxyguanosine [8-oxodG] [41,42]) and phosphorylated serine 139 histone H2A histone family member X (H2AX) (γ -H2AX) [43] in the cells. The quantitative and qualitative composition of ROS depends on the level of prooxidative (NADPH oxidase 4 [NOX4] [44] and superoxide dismutase 1 [SOD1] [45]) and antioxidative (nuclear factor erythroid 2-related factor 2 [NRF2] [46,47]) proteins. ROS can induce cell death by altering gene activity that regulates apoptosis (B-cell lymphoma 2 [Bcl-2] and Bcl-2-associated X protein [BAX] [48,49]) and autophagy (light chain 3 [LC3] [50]). For comparison, along with SatIII (1) content, we monitored the contents of two more kinds of genomic tandem repeats: telomere repeat (TR) and ribosomal repeat (rDNA) in the DNA isolated from the cells. Second, we determined if there was an association between

the SatIII (1) content and SatIII (1) transcript amount in the HSFs under stress induced by the long-term growth of confluent cells without medium replacement or by heat shock. We also compared the transcript levels of the two SatIII fractions (1q and 9q) during normal culture growth and under stress.

2. Materials and Methods

2.1 Participants

Primary adult HSFs from healthy controls (n = 5) and SZ patients (n = 5) were obtained from the Research Centre for Medical Genetics. A description of the five healthy subjects and the five SZ patients, who were the primary donors of skin cells, is presented in Table 1. The examination was conducted in the round-the-clock inpatient units of N.A. Alekseev Clinical Psychiatric Hospital No. 1 (Moscow, Russia), where the patients received standard psychiatric care. The skin samples were obtained from SZ cases with a long-term continuous form of schizophrenia. Each patient had been taking standard antipsychotics for several years (e.g., haloperidol, aminazin, risperidone, seroquel, olanzapin). Four of the five patients had nearest relatives with the same disease.

The control skin sample donors were staff members of the Research Centre for Medical 100 Genetics. They were apparently healthy, took no pharmaceuticals, and had no mental problems or relatives with mental disorders.

2.2 Cell Cultures

The cells were maintained in Dulbecco's Modified Eagle Medium supplemented with 10% fetal bovine serum (HyClone Laboratories, Logan, UT, USA), 2 mM glutamine, 50 U/mL penicillin, and 50 μ g/mL streptomycin at 37 °C in a 5% CO₂ incubator. All of the experiments were performed using cells from passage 4. Cultures with less than 2% of cells in the S phase were considered confluent. In general, cells reached confluence after 3–4 days of plating. This was marked as Day 1 of the experiment.

2.3 Ethical Approval for the Use of Cultured Human Cells

The study was carried out in accordance with the latest version of the Declaration of Helsinki and was approved by the Independent Interdisciplinary Ethics Committee on Ethical Review for Clinical Studies (Protocol No. 4 dated

March 15, 2019 for the scientific minimally interventional study “Molecular and neurophysiological markers of endogenous human psychoses”). All participants provided written informed consent to participate in the study after the procedures had been completely explained.

2.4 DNA Isolation from HSFs

To isolate the DNA, we used a standard method as previously described [51]. Briefly, 2 mL of the solution (2% sodium lauryl sarcosylate, 0.04 M EDTA, and 150 µg/mL RNase A; Sigma, St. Louis, MO, USA) was added to the cell mass for 45 min (37 °C) and then treated with proteinase K (200 µg/mL; Promega, Madison, WI, USA) for 24 h at 37 °C. The lysates were extracted with an equal volume of phenol, phenol/chloroform/isoamyl alcohol (25:24:1) and chloroform/isoamyl alcohol (24:1). DNA was precipitated by adding 1/10 the volume of 3 M sodium acetate (pH 5.2) and a 2.5-fold volume of ice-cold ethanol. DNA was collected by centrifugation (10,000 ×g for 15 min at 4 °C), washed with 70% ethanol (v/v), and dissolved in water. DNA concentration was measured in two steps, as described earlier [51]. The final DNA quantification was performed fluorometrically using PicoGreen dsDNA Quantification Reagent (Invitrogen, Carlsbad, CA, USA). The DNA concentration in a sample was calculated according to a standard curve for DNA. We used the Enspire Multimode Microplate Reader (PerkinElmer, Turku, Finland) at $\lambda_{\text{ex}} = 488 \text{ nm}$ and $\lambda_{\text{em}} = 528 \text{ nm}$.

2.5 Nonradioactive Quantitative Hybridization

The nonradioactive quantitative hybridization (NQH) method is based on the complementary hybridization of DNA immobilized on a filter with a biotin-labeled DNA probe. NQH was used for the quantification of f-SatIII, TR, and rDNA repeats, as previously detailed without modification [52,53] and Supplements of [39]. Five reference DNA probes with a known repeat content were applied to the same filter. After hybridization and biotin detection using the streptavidin-alkaline phosphatase conjugate (BCIP and nitro blue tetrazolium substrates), the filter was scanned and the spot signal intensity was measured using a customized software pack. A calibration curve was constructed, reflecting the dependence of the signal intensity on the genome's repeat copy number. The relative standard error for NQH was $5 \pm 2\%$. The major overall error of the experiment was contributed to by the step of isolating DNA from the cells. The total standard error was $11 \pm 7\%$. The DNA probe for SatIII (1) quantification was a 1.77-kb cloned EcoRI fragment of human satellite DNA [1] labeled with biotin-11-dUTP using nick translation. Dr. Cook (Medical Research Council, Edinburgh, UK) kindly supplied the human chromosome lql2-specific repetitive satellite DNA probe pUC1.77. The DNA probe for rDNA quantification contains rDNA sequences (5836 bp) cloned into an EcoRI site of the pBR322 vector. The rDNA fragment covered posi-

tions from –515 to 5321 of the human rDNA (GenBank accession No. U13369). DNA Probe used for the detection of the human TR was biotin-(TTAGGG)₇. Syntol (Moscow, Russia) performed the synthesis and biotin labeling of the oligo probe.

2.6 Flow Cytometry Analysis

Cells were analyzed using the CytoFLEX S flow cytometer (Beckman Coulter, Brea, CA, USA). HSFs were grown in 60 mm dishes. Prior to flow cytometry analysis (FCA), cells were washed with Versene solution and treated with 0.25% trypsin under light microscope observation. Then the cells were transferred to Eppendorf tubes, washed with culture medium, centrifuged, and resuspended in phosphate-buffered saline (PBS). Staining the cells with antibodies was performed as previously described [54]. Briefly, to fix the cells, paraformaldehyde (PFA; Sigma, Kawasaki, Japan) was added (3% at 37 °C for 10 min). Then the cells were washed three times with 0.5% bovine serum albumin-PBS and permeabilized with 0.1% Triton X-100 (Sigma) in PBS. Cells ($\sim 50 \times 10^3$) were stained with the following antibodies: NRF2-FITC (bs1074r-fitc; Bioss Inc., Boston, MA, USA), 8-oxodG-PE (sc-393871 PE; Santa Cruz Biotechnology, Inc., Santa Cruz, CA, USA), NOX4-PC5.5 (bs-1091r-cy5-5; Bioss Inc.), γ H2AX-pb450 (nb100-384AF405; Novus Biologicals LLC, Centennial, CO, USA), SOD1-PE (sc-11407 and rabbit IgG-PE sc-3753; Santa Cruz), BAX-PE (rabbit Nb120-7977; Novus Biologicals), secondary mouse anti-rabbit IgG-PE (sc-3753; Santa Cruz), A350-BCL2 (bs-15533r-a350; Bioss Antibodies Inc. Woburn, USA), LC3DyLight 488 (NB100-2220G; Novus Biologicals). To quantify the background fluorescence, we stained a portion of the cells with secondary FITC (PE, PC5.5, pb450, DAPI)-conjugated antibodies only. Primary data are presented as median signal intensities minus signal background values. For a more convenient presentation of the data, the values of the medians of FL-signal were normalized to the maximum FL-signal value in the sample ($n = 10$). The relative standard error of the FCA was $4 \pm 2\%$.

2.7 ROS Assay

The fluorescent assay was applied for ROS quantification in HSFs in the format of a 96-well tablet reader at $\lambda_{\text{ex}} = 488 \text{ nm}$ and $\lambda_{\text{em}} = 528 \text{ nm}$ (Enspire, PerkinElmer, Turku, Finland). The medium was replaced with 5 µm H2DCFH-DA (Molecular Probes/Invitrogen, Thermo Fisher Scientific, Waltham, MA, USA) in PBS, and a fluorescence intensity was measured at 37 °C. Eight (4×2) measurements were made for each DNA sample and 16 for the control. The slope of the line (k), which reflects the dependence of the fluorescence intensity on time, characterizes the ROS content in HSFs. This method allows quantification of the total ROS amount in HSFs (intracellular) and in the extracellular medium. For the intracellular ROS assay (i.e.,

only in the cells), FCA was applied. The medium was replaced with 5 μM H2DCFH-DA in PBS for 1 h at 37 °C. Prior to FCA, cells were washed with Versene solution and treated with 0.25% trypsin under light microscope observation. Then the cells were transferred to Eppendorf tubes, washed with PBS, centrifuged, and resuspended in PBS.

2.8 Quantitative Polymerase Chain Reaction

Isolation of the RNA was performed using the RNeasy Mini kit (Qiagen, Hilden, Germany). RNA was quantified using the Quant-iTRiboGreen RNA Reagent (Molecular Biology, Göttingen, Germany) on a multimode plate reader (EnSpire; PerkinElmer) at $\lambda_{\text{em}} = 487 \text{ nm}$, $\lambda_{\text{fl}} = 524 \text{ nm}$. The RNA samples were further treated with DNase I to remove possible trace amounts of DNA. After DNase I treatment, RNA samples were reverse transcribed using the Reverse Transcriptase Kit (Sileks, Moscow, Russia). PCR was conducted with specific primers and SYBR Green intercalating dye on the StepOnePlus Real-Time Polymerase Chain Reaction (PCR) System (Applied Biosystems, Foster City, CA, USA). The primers were selected and synthesized by Evrogen (Moscow, Russia). The internal standard was the *TATA box-binding protein* gene. For the RNASATIII assay, primers described in [34] were applied. In each series of experiments, RNA samples treated with DNase I were used as a negative control. The PCR reaction mixture in a volume of 25 μL consisted of 2.5 μL PCR buffer (700 mmol/L Tris-HCl, pH 8.6); 166 mmol/L ammonium sulfate, 35 mmol/L MgCl_2 , 2 μL of 1.5 mmol/L dNTP solution; and 1 μL of 30 pmol/L primer solution, cDNA. PCR conditions were chosen individually for each primer pair. After denaturation for 4 min at 95 °C, 40 amplification cycles were performed in the following order: 94 °C for 20 s, 56–62 °C for 30 s, 72 °C for 30 s, and 72 °C for 5 min. The data were processed using a calibration plot with a resultant error of 2%.

2.9 Fluorescence Microscopy

The Axio Scope.A1 microscope (Carl Zeiss, Oberkochen, Germany) was used for fluorescence microscopy. For γH2AX detection, cells were washed three times with PBS, fixed for 20 min in 3% PFA at 4 °C, washed with PBS, and incubated for 4 h at 4 °C with γH2AX -FITC antibodies. After washing with 0.01% Triton X-100 in PBS, HSFs were washed with PBS and stained with 2 $\mu\text{g}/\text{mL}$ DAPI.

For fluorescence *in situ* hybridization (FISH), the HSFs in slide flasks were washed with PBS. The slides were removed and placed for 10 min into a cold fixation solution. After the procedure was repeated three times, the slides were dried and subjected to FISH. Before hybridization, the slides were treated with RNase A (100 $\mu\text{g}/\text{mL}$). Hybridization was conducted using the protocol and solutions from Abbott Laboratories (Abbott Park, IL, USA) in the Statspin ThermoBrite Slide Denaturation and Hybridization System (Abbott Molecular Inc., Des Plaines, IL, USA) at

42°. Nuclei were stained with propidium iodide. The f-SatIII FISH probe was a 1.77-kb-cloned EcoRI fragment of human satellite DNA [54]. Labeling of plasmid pUC1.77 was performed using nick translation with the CGH Nick Translation Kit (Abbott Molecular) according to the manufacturer's protocol.

2.10 Statistical Analyses

Each test was repeated in triplicate. In FCA, the medians of the signal intensities were analyzed. The significance of the observed differences was analyzed using the nonparametric Mann–Whitney test (p) and Kolmogorov–Smirnov test (D and α). Spearman analysis (R_s , p) was used to analyze correlations between the two parameters. $p < 0.01$ and $\alpha < 0.04$ were considered statistically significant. The data were analyzed with Microsoft Excel and Office (Microsoft, Redmond, WA, USA), StatPlus2007 Professional software (<http://www.analystsoft.com> accessed on March 19, 2022), and StatGraphics (Statgraphics Technologies, The Plains, VA, USA).

3. Results

The HSFs of healthy controls (hc-HSFs, K1-K5) and SZ patients (sz-HSFs, SZ1–SZ5) were studied. After inoculation, sz-HSFs and hc-HSFs were cultured until confluence (3–4 days). Cultures with less than 1% of cells in the S phase were considered confluent. This was marked as Day 1 (control) of the experiment.

3.1 CNVs of the Three Tandem Repeats in Confluent HSFs

Fig. 1 shows the content data of the three tandem repeats (SatIII (1), TR, and rDNA) in DNA isolated from cells that had reached confluence (control). For reference, the contents of the repeats in actively proliferating cell culture 2 days before the confluent state (–2 days) were also given.

In proliferating HSFs, the SatIII (1) content in DNA varied from 11 pg/ng DNA (3SZ) up to 16 pg/ng (1SZ). Proliferating sz-HSFs and hc-HSFs did not significantly differ by SatIII (1) content in DNA (Fig. 1A,a1). The SatIII (1) content in the DNA of confluent cells varied from 11 pg/ng (4K) up to 36 pg/ng (1SZ) (Fig. 1A,a1). The DNA isolated from confluent sz-HSFs contained more SatIII (1) repeats than DNA isolated from hc-HSFs ($D = 0.8$, $\alpha = 0.036$; $p < 0.01$).

The TR content in DNA varied from 71 pg/ μg DNA (1SZ) up to 335 pg/ μg (4K) (Fig. 1A,a2), corresponding with the average LTL, approximately 2 to 7 kb. Hc-HSFs carried more copies of TR ($D = 0.8$, $\alpha = 0.036$; $p < 0.01$) in their genomes than sz-HSFs, suggesting longer telomeres in hc-HSFs. A comparison of confluent cell DNA (control) to DNA isolated from actively proliferating cells (–2 days) showed a slight decrease of TR contents in DNA of confluent sz-HSFs. The TR content in DNA of the confluent HSFs negatively correlated (Fig. 1A,a4) with the SatIII (1) content ($R_s = -0.88$, $p < 0.001$, $n = 10$).

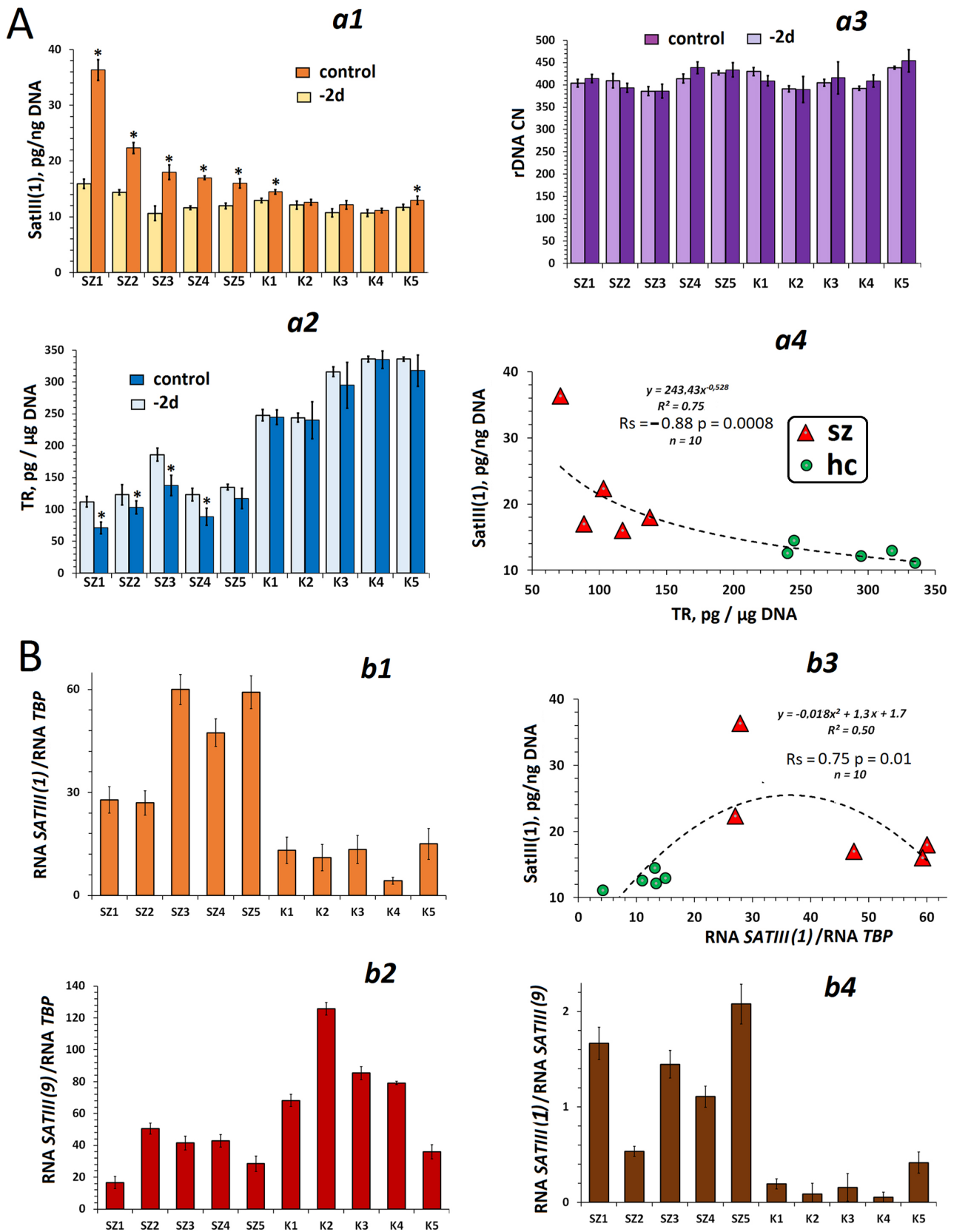


Fig. 1. CNVs of the three tandem repeats and RNASATIII in the HSFs. (A) SatIII (1) (a1), TR (a2) and rDNA (a3) content in confluent (control) and proliferating (–2 d) HSFs. (a4) An association between SatIII (1) and TR contents in confluent HSFs. (B) RNASATIII (1) (b1) and RNASATIII (9) (b2) content in confluent HSFs. (b3) An association between SatIII (1) content and RNASATIII (1) content. (b4) RNASATIII (1)/RNASATIII (9) ratio in confluent HSFs. * - the difference is statistically significant.

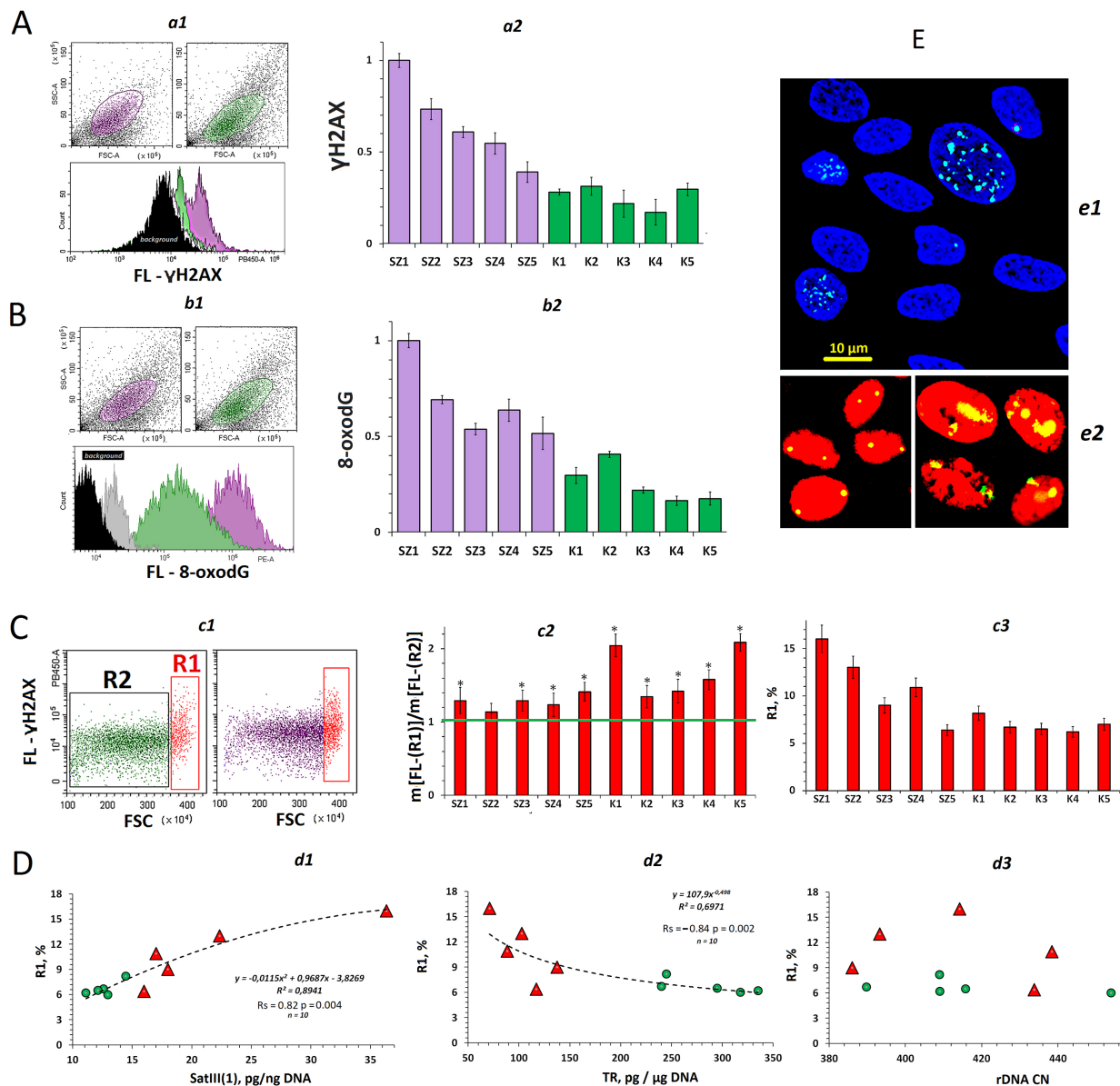


Fig. 2. An analysis of DNA damage in human skin fibroblasts (HSFs). (A) (a1) An example of FCA for γ H2AX detection in SZ1 and K4. (a2) Index γ H2AX. (B) (b1) An example of FCA for 8-oxodG detection in SZ1 and K4. (b2) Index 8-oxodG. (C) (c1) Plot γ H2AX - FSC for SZ1 and K4. (c2) FL- γ H2AX median ratio for areas R1 and R2. (c3) The R1 subset fraction size. (D) Dependence of R1 fraction size on the contents of SatIII (1) (d1), TR (d2) or rDNA (d3). (E) (e1) An example of γ H2AX-FITC distribution in the nuclei (stained with DAPI). (e2) FISH for nuclei with small and large size (stained with PrI). * - the difference is statistically significant.

The numbers of rDNA copies in HSFs varied from 386 (3SZ) up to 454(5K). Sz-HSFs and hc-HSFs did not differ by rDNA abundance in the cellular DNA (Fig. 1A,a3). This index did not change during cell cultivation. Thus, in the process of culturing HSFs to a confluent state, the SatIII (1) content in the isolated DNA increases. One of the possible reasons for the SatIII (1) content increase may be an increase in the amount of RNA *SATIII (1)*.

3.2 RNASATIII Content in Confluent HSFs

In confluent cells, SatIII (1) repeats were transcribed, as evidenced by the detected amounts of RNASATIII (1).

SatIII (1) transcription intensity in sz-HSFs was higher ($D = 0.8$, $\alpha = 0.036$; $p < 0.01$) than that in hc-HSFs (Fig. 1B,b1). There was a positive correlation between the level of RNASATIII and the amount of SatIII (1) DNA (Fig. 1B,b3). For comparison, we quantified the transcription level of another satellite III, which is localized in the pericentromeric region of chromosome 9. In contrast to RNASATIII (1), the RNASATIII (9) content in sz-HSFs was lower ($D = 0.8$, $\alpha = 0.036$; $p < 0.05$) than in hc-HSFs (Fig. 1B,b2). In confluent sz-HSFs, the RNASATIII (1)/RNASATIII (9) ratio was 8-fold higher than in hc-HSFs (Fig. 1B,b4).

Thus, it was shown that the content of the SatIII (1) repeat in DNA isolated from confluent cells correlated with the content of RNASATIII in RNA isolated from the same cells. Stress is an inducer of SatIII (1) transcription [34, 35]. To determine the level of endogenous stress that could induce satellite transcription and subsequent satellite DNA amplification, we determined some characteristics, which indicate the level of oxidative stress in the HSF pool.

3.3 Cellular DNA Damage

To estimate the double-strand DNA breaks rate in nuclear DNA, antibodies to 301 phosphorylated form of histone H2AX (γ H2AX) [43] were applied (Fig. 2A,a1). For the reader's convenience, a median value of cell signal for each HSF cell line was normalized to the maximum median value of the signal in the sample (parameter γ H2AX = $m[\text{FL-}\gamma\text{H2AX}]_i/m[\text{FL-}\gamma\text{H2AX}]_{\text{max}}$). The amounts of γ H2AX in sz-HSFs were higher than those in hc-HSFs ($D = 0.8$, $\alpha = 0.036$; $p < 0.01$). The maximum damage degree was observed for SZ1, whereas the minimum one was observed for K4 (Fig. 2A,a2).

An analysis of the dependence of γ H2AX on FSC parameter, which indicates the cell size, allowed us to distinguish the cell subset R1 (Fig. 2C,c1–c3 and 2E,e1) with large sizes and relatively high, compared to the other cells, level of the DNA damage marker. This fraction varied in the confluent HSFs from 6% to 16% and correlated positively with SatIII (1) repeat content in the DNA ($R_s = +0.82$, $p = 0.0038$, $n = 10$), while correlated negatively ($R_s = -0.84$, $p = 0.0022$, $n = 10$) with the TR abundance (Fig. 2D,d1,d2). The rDNA abundance in the genome was not associated with the size of R1 fraction (Fig. 2D,d3).

FISH was conducted to analyze the state of SatIII (1) repeat (Fig. 2E,e2). SatIII (1) is localized in two homologous sites of the nucleus. In cells of normal size, they are visualized as two compact spots. In large cells, the SatIII (1) signal area is much larger, suggesting both chromatin decondensation and an increased total copy number of the repeat in such cells.

The DNA oxidation degree was tested using antibodies against an oxidation marker 8-oxodG (Fig. 2B,b1). The 8-oxodG rate (parameter 8-oxodG = $m[\text{FL-8-oxodG}]_i/m[\text{FL-8-oxodG}]_{\text{max}}$) was higher in sz-HSFs than in hc-HSFs ($D = 0.8$, $\alpha = 0.036$; $p < 0.01$). The maximum DNA oxidation degree was observed for SZ1, and the minimum one was observed for K4 (Fig. 2B).

Thus, the oxidative modification seems to be the major cause of DNA breaks, resulting from the high content of endogenous ROS in HSF cell pools. The ROS amount depends on the balance of pro- and antioxidant enzyme activity. We assayed the ROS amount and the contents of three proteins (NOX4, SOD1, and NRF2) that regulate ROS abundance in the cell.

3.4 ROS Abundance in Confluent HSFs

The ROS were quantified using $\text{H}_2\text{DCFH-DA}$ chemical reagent and a tablet reader (Fig. 3A). To estimate the ROS amount, the synthesis rate constant DCF (k) was determined in confluent sz-HSFs after the reagent had been added. The k value for sz-HSFs was considerably higher than that for hc-HSFs, suggesting a higher ROS level in the cells derived from SZ patients (Fig. 3A,a1,a2).

The distribution of unfixed cells by ROS amount was estimated using FCA (Fig. 3A,a3). The HSF cell pool appeared to be heterogeneous by this parameter. Three fractions could be distinguished. R1 were large cells with an elevated ROS content. R2 and R3 were cells of approximately the same normal size, but with different ROS levels.

One way to determine an increase in ROS is *NOX4* gene activity (Fig. 3B). The amount of *RNA_{NOX4}* was on the average more in sz-HSFs than in hc-HSFs ($p < 0.05$). 2K line cells were an exclusion showing a higher *RNA_{NOX4}* level than the other hc-HSFs (Fig. 4B,b1). *NOX4* protein content as determined using FCA (*NOX4* index) was positively correlated with *RNA_{NOX4}* content ($R_s = +0.75$, $p = 0.012$, $n = 10$). The *NOX4* index was higher for sz-HSFs than for hc-HSFs ($D = 0.8$, $\alpha = 0.036$; $p < 0.01$).

The amounts of RNA transcribed from the *NFE2L2* gene encoding NRF2 transcription factor were equal in sz-HSFs and hc-HSFs ($p > 0.1$; Fig. 3C,c1). However, NRF2 protein content (NRF2 index) was slightly increased (differences were not significant) in sz-HSFs compared to hc-HSFs (Fig. 3C,c2,c3). The NRF2 index did not correlate with *RNA_{NFE2L2}* amount.

The mRNA and protein levels of SOD1 (SOD1 index) were the same in sz-HSFs and hc-HSFs ($p > 0.1$; Fig. 3D). K5 line cells contained the maximum level of the protein. The SOD1 index did not correlate with *RNA_{SOD1}* amount.

3.5 Apoptosis and Autophagy Gene Expression

We found no significant differences in the RNA and protein levels of *BAX* and *BCL2* between sz-HSFs and hc-HSFs (Fig. 4A–C). The maximum *BAX* index was observed for SZ1, whereas the minimum one was observed for K3 and K4 (Fig. 4A,a3). A *BAX/BCL2* ratio, which represents the apoptosis intensity [55], was higher for sz-HSFs than for hc-HSFs ($p < 0.015$), with the exception of the K5 cell line. For K5, high values of *RNA_{BAX}/RNA_{BCL2}* and *BAX/BCL2* indices were observed (Fig. 4C).

In lines SZ1–SZ4, a considerable increase in *ATG16L1* RNA was found (Fig. 4D,d1). The *ATG16L1* gene governs the process of autophagy. We determined the amount of protein LC3, which indicates the autophagy intensity in the cells (Fig. 4D,d2,d3). For sz-HSFs, the LC3 index was higher than that for hc-HSFs ($D = 0.8$, $\alpha = 0.036$; $p < 0.01$).

The large size cell fraction (R1) was enriched with cells with a high level of LC3 protein (Fig. 4E,e1,e2). A joint analysis of levels of γ H2AX and LC3 in the same cells

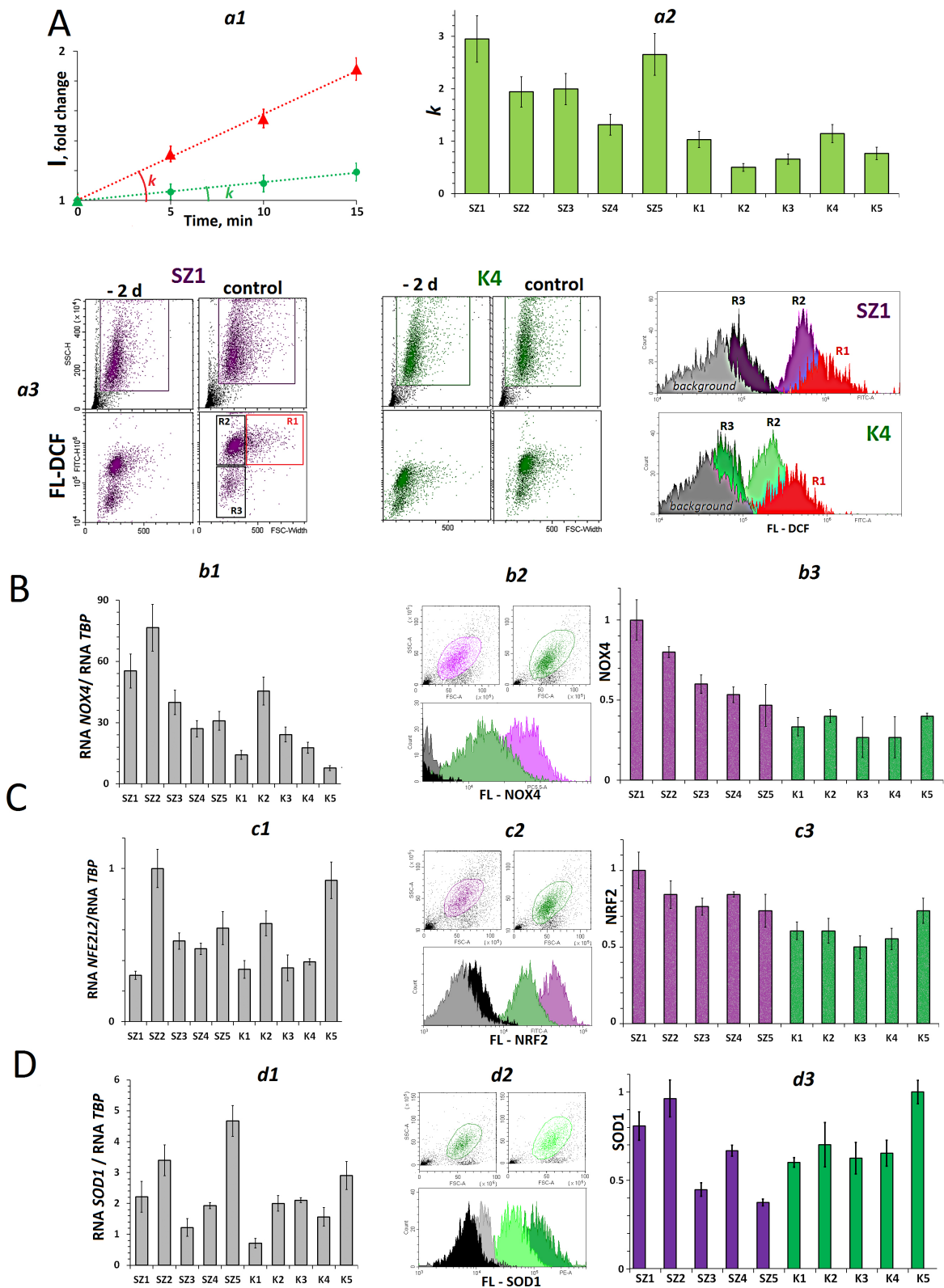


Fig. 3. Reactive oxygen species (ROS) level in the HSFs. (A) (*a1*) An example of ROS detection in SZ1 (red) and K4 (green) with H₂DCFH-DA. The reader performs measurements of signal intensity every 5 min. (*a2*) k DCF for all HSFs. (*a3*) An example of FCA for ROS detection in SZ1 and K4. (B) (*b1*) RNANOX4 amount in the HSFs. (*b2*) An example of FCA for NOX4 detection in SZ1 and K4. (*b3*) Index NOX4. (C) (*c1*) RNANFE2L2 amount in the HSFs. (*c2*) An example of FCA for NOX4 detection in SZ1 and K4. (*c3*) Index NRF2. (D) (*d1*) RNASOD1 amount in the HSFs. (*d2*) An example of FCA for SOD1 detection in SZ1 and K4. (*d3*) Index SOD1.

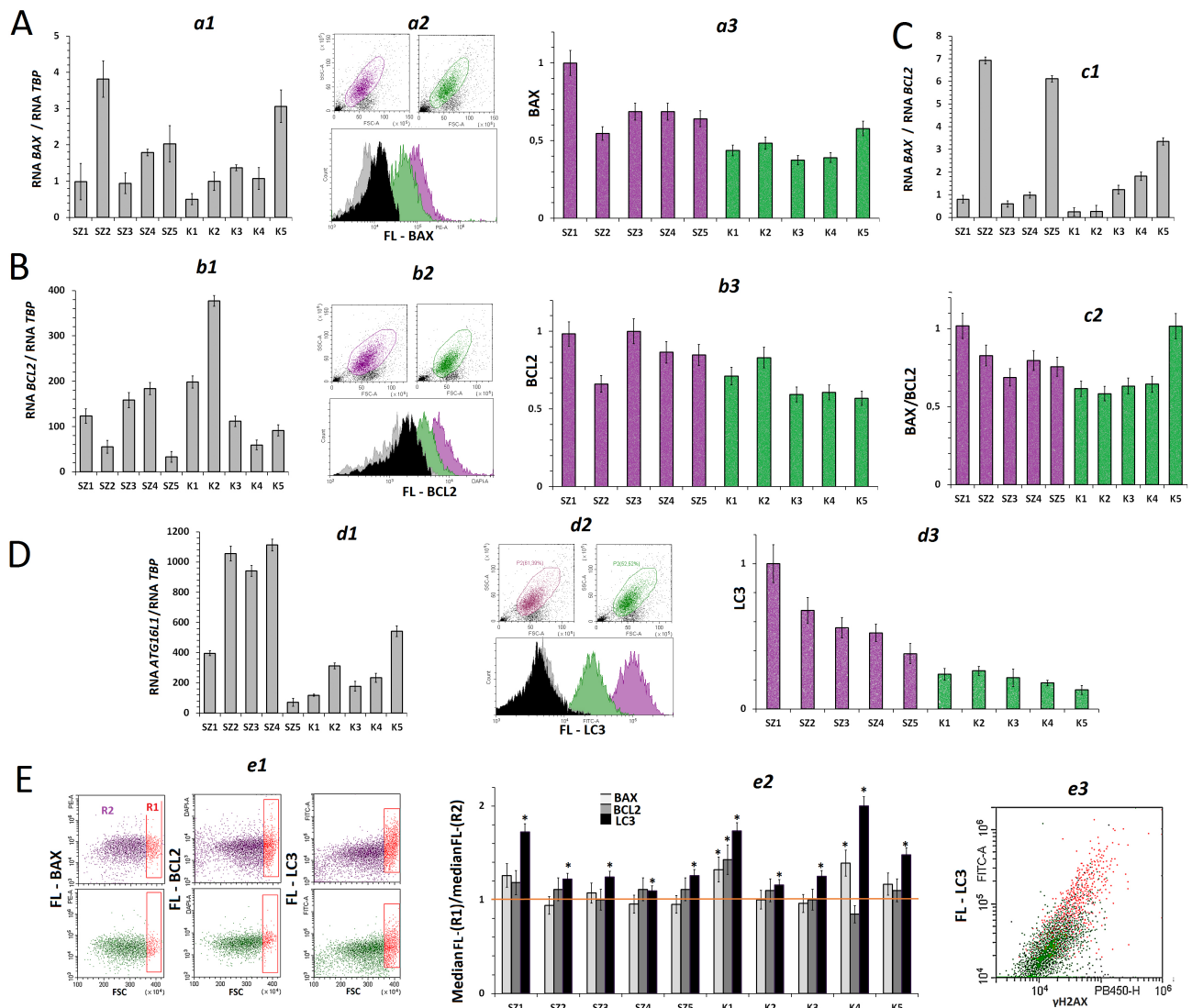


Fig. 4. The apoptosis and autophagy indicators in HSFs. (A) (a1) RNABAX1 amount in the HSFs. (a2) An example of FCA for BAX detection in SZ1 and K4. (a3) BAX indices. (B) (b1) RNABCL2 amount in the HSFs. (b2) An example of FCA for BCL2 detection in SZ1 and K4. (b3) BCL2 indices. (C) (c1) RNABAX1/RNABCL2 ratio in the HSFs. (c2) BAX1/BCL2 ratio in the HSFs. (D) (d1) RNAATG1601 amount in the HSFs. (d2) An example of FCA for LC3 detection in SZ1 and K4. (d3) Index LC3. (E) (e1) Plots FL-(BAX, BCL2, LC3) – FSC. R1 area is framed. (e2) FL-(BAX, BCL2, LC3) median ratio for R1 and R2 areas (* - the difference is statistically significant). (e3) Plot FL-LC3 – γ H2AX for SZ1 (red) and K4 (green).

showed that the process of autophagy was activated in cells with a high DNA damage degree, which were part of fraction R1 (Fig. 4E,e3).

3.6 Dependence of SatIII (1) Contents in DNA on the Cell Characteristics

Fig. 5 shows the dependence of SatIII (1) content on the abovementioned characteristics of the cell lines. The SatIII (1) repeat abundance was positively correlated with the levels of DNA damage markers (γ H2AX and 8-oxodG), proteins that modulate ROS amount (NOX4 and NRF2), and indices that represent the apoptosis and autophagy intensity (BAX and LC3). The largest SatIII (1) copy number, as measured for DNA derived from SZ1 cells, corresponds

to the maximum values of the parameters that display the level of oxidative stress. A positive correlation between the stress indicators and the content of the SatIII (1) repeat in DNA was also preserved in the individual groups (Fig. 5). Thus, we showed that a high SatIII (1) content in cell DNA is associated with exaggerated endogenous oxidative stress in the cell population.

3.7 Changes in SatIII (1) Content in DNA Under Increased Stress

3.7.1 Confluent Cell Cultivation without Medium Replacement

A 4-day cultivation of confluent HSFs without medium replacement was followed by a decrease of SatIII

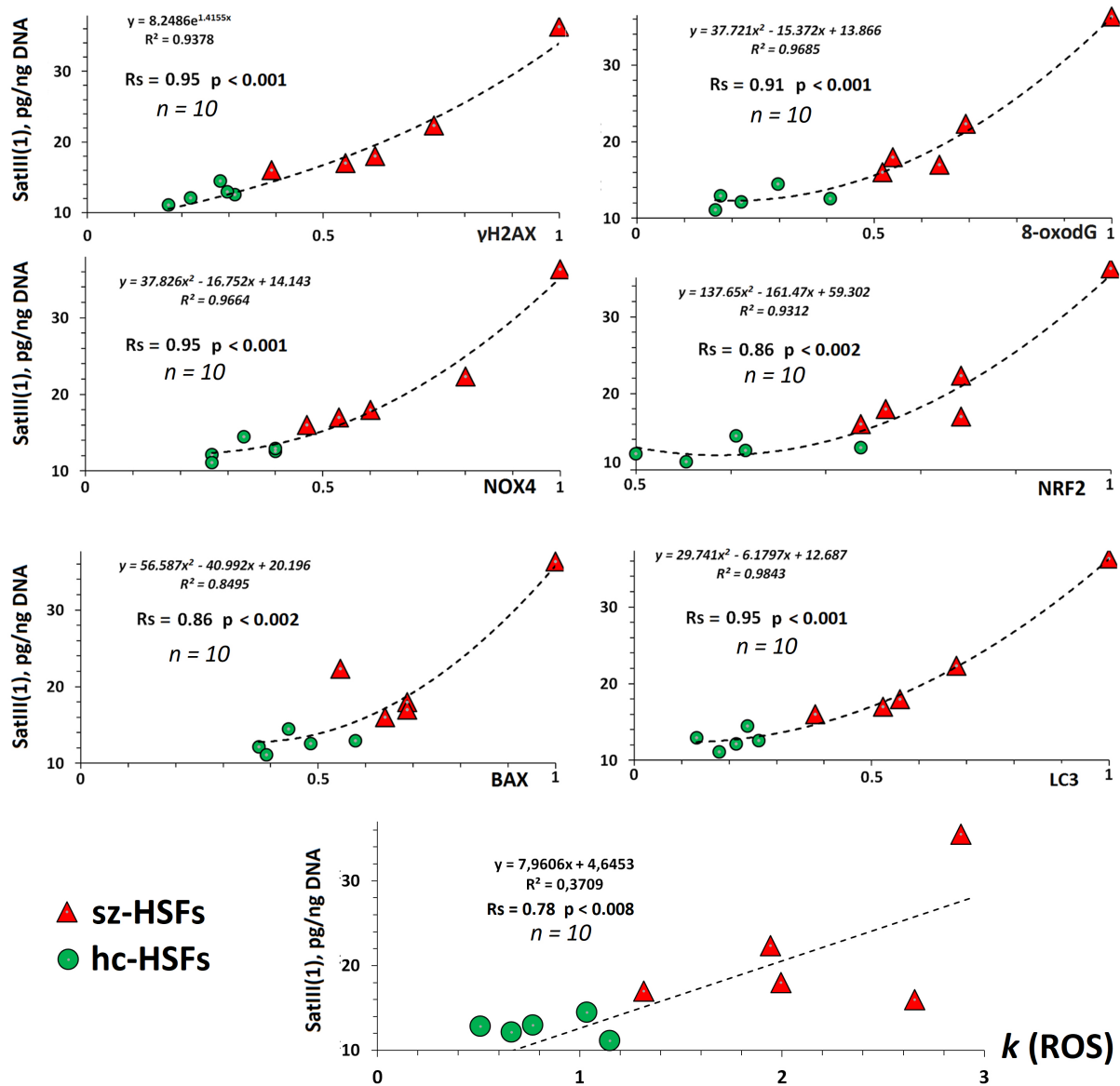


Fig. 5. Dependence of SatIII (1) content in DNA isolated from confluent fibroblasts on the values of indices reflecting the level of endogenous oxidative stress in the HSFs.

(1) repeat content in the DNA of all sz-HSFs by a factor of 1.5 to 4, with the maximum effect observed for SZ1 (Fig. 6A,a1,a3). In hc-HSFs, SatIII (1) copy numbers did not reduce (K1) or reduced them by a factor of 1.1 to 1.6 (i.e., to a lesser degree than in szHSFs). Unlike SatIII (1) repeats, the abundance of TR in HSF DNAs was increased or remained unchanged (K1). Long-term HSF growth without medium replacement was accompanied by no changes in rDNA content (Fig. 6B,b1). We explored changes in RNASATIII amount after 2 days of confluent cell growth. The RNASATIII (1) amount in RNA isolated from the cells increased by a factor of 1.2 (K2) to 140 (K3) (Fig. 6C,c1,c3). By contrast, the RNASATIII (9) amount decreased by a factor of 1.5 (SZ5) to 6 (K2) (Fig. 6D,d1,d3). The RNASATIII (1)/RNASATIII (9) ratio increased by a factor of 2 (SZ5) to 400 (K3). Thus, long-term confluent

cell cultivation induced a decrease in the SatIII (1) content in DNA together with a simultaneous increase in the amount of RNASATIII (1) in RNA isolated from the cells.

3.7.2 Stress Induced by Incubating HSFs at 42 °C

The cells were incubated for 1 h at 42 °C and then at 37 °C for 5 h. A decrease in SatIII (1) repeat content was observed in the DNA of each HSF by a factor of 1.1 (K1) to 2.8 (SZ1) (Fig. 6A,a2,a3). The copy number of TR in nine HSFs increased by a factor of 1.1 to 1.6. In K3, we observed a 1.4-fold reduction of the repeat abundance (Fig. 6B,b2,b3). The rDNA content in the cellular DNA did not change (Fig. 6B,b1). A heat shock induced an expected [14] increase of RNASATIII (9) amount by a factor of 1.4 (SZ1) to 120 (SZ4) (Fig. 6D,d2,d3). On the contrary, RNASATIII (1) amount decreased in each HSF

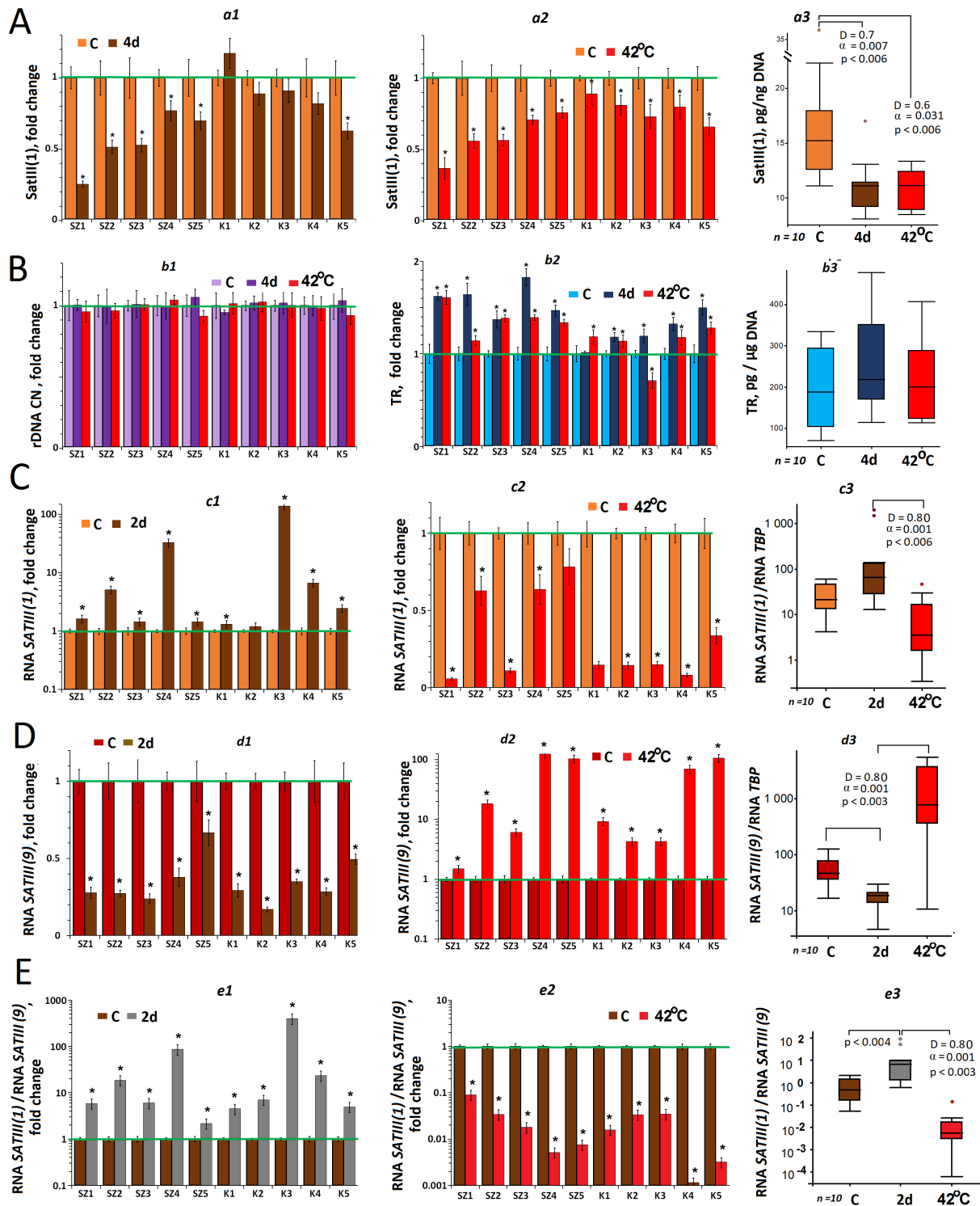


Fig. 6. Stress-induced changes in the contents (copy numbers) of the three tandem repeats and RNASATIII in the HSF cell lines studied. (A) Changes in SatIII (1) content during the cultivation of confluent HSFs without medium replacement (*a1*, *a3*) and after heat shock (*a2*, *a3*). (B) Changes in rDNA content (*b1*) and TR content (*b2*, *b3*) during the cultivation of confluent HSFs without medium replacement and after heat shock. (C) Changes in RNASATIII (1) content during the cultivation of confluent HSFs without medium replacement (*c1*, *c3*) and after heat shock (*c2*, *c3*). (D) Changes in RNASATIII (9) content during the cultivation of confluent HSFs without medium replacement (*d1*, *d3*) and after heat shock (*d2*, *d3*). (E) Changes of RNASATIII (1)/RNASATIII (9) ratio during the cultivation of confluent HSFs without medium replacement (*e1*) and after heat shock (*e2*, *e3*). * - the difference is statistically significant.

line by a factor of 1.3 (SZ5) to 17 (SZ1) (Fig. 6C,e2,e3). The RNASATIII (1)/RNASATIII (9) ratio was reduced by a factor of 11 (SZ1) to 400 (K4) after the heat shock (Fig. 6E,e2,e3). Thus, heat shock in the confluent cells induced a decrease in SatIII (1) content in DNA followed by a decrease in the amount of RNASATIII (1) in RNA isolated from the cells.

4. Discussion

The aim of this study was to analyze the variation in SatIII (1) abundance in cultured HSFs at early passages depending on the levels of endogenous and exogenous stress. To this end, we selected HSFs from healthy individuals and HSFs from chronic SZ patients. We chose sz-HSFs because it is known that patients with schizophrenia experience systemic oxidative stress [56]; therefore, the cells of SZ patients should potentially have a higher level of ROS. This assumption was confirmed, as sz-HSFs produced more ROS after they reached confluence, compared to cells from healthy skin donors (Fig. 3A). A higher ROS level in sz-HSFs correlated with a higher degree of DNA damage (Fig. 2) and higher contents of the pro-oxidant protein NOX4 (Fig. 3), proapoptotic protein BAX, and protein LC3 involved in the autophagy process (Fig. 4). Previously, elevated NOX4 protein is detected in the blood lymphocytes and brain cells of SZ patients [57,58]. The DNA damage degree is also increased in both the primary and cultured cells of SZ patients [59]. The process of apoptosis is more active in SZ patients than in healthy controls [60].

Thus, we studied two groups of HSFs with different levels of endogenous ROS. The high level of ROS in the sz-HSFs is apparently due to the genetic characteristics associated with the development of the disease. In addition, patients had been taking antipsychotics for a long period of time, which could potentially cause epigenetic changes in skin cells that caused increased levels of stress or/and high SatIII (1) content. However, there are no data in the literature on the effects of antipsychotics *in vivo* on cultured skin cells outside the body. By contrast, fibroblasts are considered a convenient model that allows the assessment of genetic changes in the absence of endogenous influence of the body's environment, including the influence of therapy [61].

We analyzed the effects of three types of cell culture conditions on the repeat contents in cellular DNA.

4.1 Effects of Endogenous ROS Levels on SatIII (1) CNVs in HSFs

A high level of oxidative stress and DNA damage markers in HSFs was associated with increased SatIII (1) repeat content in the DNA isolated from the confluent cells (Fig. 5). An analysis of histograms of cell distribution by γ H2AX marker content showed that many cells of sz-HSFs had a high marker content, but especially increased γ H2AX was observed in a small subset of large-size cells. The frac-

tion of such cells was correlated with the SatIII (1) content in the total DNA isolated from the cells (Fig. 2). The data obtained using FISH suggested that in these cells, the SatIII (1) repeat copy numbers were increased and/or chromatin decondensation occurred at the site of hybridization with a probe for SatIII (1).

A high SatIII (1) content in total DNA was correlated with a low TR content (Fig. 1). Earlier, opposite changes of TR and SatIII (1) contents in the cellular DNA were revealed when studying variation of these tandem repeats during replicative senescence of five HSF lines [39], in various brain regions of a SZ patient [62] and in the research of the human blood cell response for an affective stress [63]. In every case, increased SatIII (1) content in the cellular DNA was linked to a reduced TR count.

For the SatIII (1) repeat region, DNA decondensation and demethylation were previously found at late passages, accompanied by an exaggerated transcription of SatIII (1) DNA [34]. We measured the RNASATIII (1) levels in HSFs (Fig. 1). The transcript amount in sz-HSFs exceeded that in hc-HSFs, correlating with a higher SatIII (1) repeat content in sz-HSFs. An increased level of satellite transcription under conditions of endogenous oxidative stress may be one of the reasons for the increase in the content of the SatIII (1) repeat in some cells of the population.

One report [34] also showed that senescence was not accompanied by the transcription of SatIII (9) repeats localized in the pericentromeric region of chromosome 9, in contrast to SatIII (1). An assay of RNASATIII (9) showed that the amount of the transcript was decreased in sz-HSFs compared to hc-HSFs. The activation of SatIII (1) transcription was accompanied by a decrease in SatIII (9) transcript level (Fig. 1B,b4). We previously observed a similar phenomenon when studying the effects of cell exposure to ionizing radiation [35].

In total, our findings suggest that under the stress caused by endogenous factors, an increase in SatIII (1) copy numbers occurs in cells with a low count of TRs. Seemingly, these cells undergo the biggest ROS impact. Telomere shortening is associated with heterochromatin decondensation and activation of transcription from these regions. A mechanism previously proposed by Bersani *et al.* [38] may be involved in the increase of SatIII (1) cellular content under the action of stress factors. By means of reverse transcriptase, a DNA chain is synthesized from RNASATIII, and the DNA–RNA hybrids then forms, inserts into the transcribed region, and undergoes the action of DNA repair enzymes. The region 1q12 under exploration is known to be one of the most unstable chromatin sites [63]. In this chromatin region, the double-strand break repair processes are suppressed, thus increasing the chances of successful integration of the DNA–RNA hybrids into DNA [64].

The insertion of additional SatIII (1) fragments into the heterochromatin regions in some cells cannot be detected by analyzing the size of the chromatin block on

metaphase chromosomes. We previously showed that cells with an elevated SatIII (1) content are unable to respond to various impacts that require genome architecture rearrangements necessary for changing the gene expression profiles in response to stress. In particular, these cells do not respond to proliferative stimuli (i.e., cannot enter the mitosis phase). In addition, such cells fail to launch an adaptive response for an exposure to small doses of ionizing radiation [35] and perish as a result of even a weak toxic impact.

The correlation of SatIII (1) copy number with stress markers and sufficiently high SatIII (1) transcription level in HSFs suggests that even relatively young cell pools (at early passages) can accrue cells with high SatIII (1) content during cultivation, which do not divide and are not resistant to stronger types of stressor impacts. To prove this assumption, we analyzed the changes of SatIII (1) content caused by two types of stress.

4.2 Cultivation of Confluent HSFs without Medium Replacement

Cultivating cells for a long time without medium replacement is accompanied by stress resulting from a decline of nutrients in the medium and cellular debris accumulation due to apoptosis, which can induce extra ROS synthesis in living cells [65]. Four days after HSFs had reached confluency, the SatIII (1) copy numbers significantly decreased in DNA samples isolated from sz-HSFs (Fig. 6A,a1,a3). A slight decrease of SatIII (1) content also occurred in four DNA samples isolated from hc-HSFs. Simultaneously with the decrease of SatIII (1) content, an increase in TR abundance was observed in DNA isolated from HSFs (Fig. 6B,b2). The copy numbers of ribosomal repeat remained virtually unchanged in the isolated DNA (Fig. 6B,b1). The observed changes in the contents of the two repeats in DNA isolated from the cells after long-term growth without medium replacement suggest that this stress type induces death of cells with high SatIII (1) content and relatively low TR abundance in the pools of HSFs. These findings corroborate the reports of hypersensitivity of cells with high SatIII (1) contents to damaging impacts due to a blockage of the adaptive response in these cells [35].

4.3 Heat Shock Effect

The cell's response to heat shock considerably differs from its response to prolonged cultivation without medium replacement by the RNASATIII (1)/RNASATIII (9) ratio change patterns. Heat shock induced SatIII (9) transcription, as previously described [14], while the resultant amount of SatIII (1) transcripts was considerably reduced (Fig. 6C–E).

Despite the difference in the changes of transcription of different SatIII fragments under heat shock and cultivation without medium replacement, the patterns of changes in SatIII (1) and TR copy numbers in the cellular DNA were similar: while SatIII (1) repeats were reduced, the TR ar-

rays were enlarged (Fig. 6B). These data suggest a stress-induced process of death in cells with a high abundance of SatIII (1), and simultaneously, a low content of TR.

4.4 Satellite III CNV in Cultured HSFs

An integrated analysis to summarize the previous reports [35,39] and the data obtained in this study suggested a scheme of satellite III (1q12) CNV in cultured cells with different levels of endogenous ROS production (Fig. 7).

The cell pool of HSFs is heterogeneous by the copy numbers of satellite III (1q12) repeats in the cell genomes. As early as the first passages, they contain a small fraction of cells with an elevated SatIII (1) content [39]. The clones with high SatIII (1) content consist of a few cells, because the proliferative capacity of these cells is considerably abated as compared to cells harboring low SatIII (1) abundance in the genome. The amounts of TR in cells that had formed clones (dividing cell) with high and with low SatIII (1) contents did not differ [39].

The cell pool of HSFs is also heterogeneous by ROS level (Fig. 3A). In confluent HSFs, cells with high ROS content formed a subset, which was characterized by a large cell size and high DNA damage degree. The size of this cell fraction correlated with increased SatIII (1) content and decreased TR content in the DNA isolated from the whole bulk of cells. FISH data suggested that SatIII (1) content was increased, for the most part, in the cells that belonged to this fraction (Fig. 2). As previously shown, cells with the same characteristics accrued during replicative senescence [39].

An extra stress impact induces death of the cells with a high SatIII (1) content and a low TR count. Such cells are not capable of development of the adaptive response and have hypersensitivity to DNA damaging agents [35]. The abovementioned process occurs during various stress types – cultivation without medium replacement and heat shock (our study's findings), as well as exposure to ionization radiation [35]. As a result, the after-stress DNA isolated from HSFs had a decreased SatIII (1) content, and to a lesser degree, an increased TR content (Fig. 6). Perhaps, the cells with high SatIII (1) content and low TR content dying under exposure to small radiation doses, are a source of extracellular DNA fragments, which induce a bystander effect and an adaptive response in the other (surviving) cells of the cell pool. Existence of such a subset in every cell pool was hypothesized earlier [66].

In vivo, the body inevitably undergoes the environmental stress impact, sooner or later. Thus, the SatIII (1) content in the total DNA passes a cycle of an increase and a decrease, and the TR content passes a similar, but phase-shifted cycle, as shown in Fig. 7. The figure shows one oscillation, but provided that cell pools are regularly renewed in a living body and the stresses are also repeated from time to time all over the lifetime, one can hypothesize that the oscillations are recurrent *in vivo*. This speculation had be-

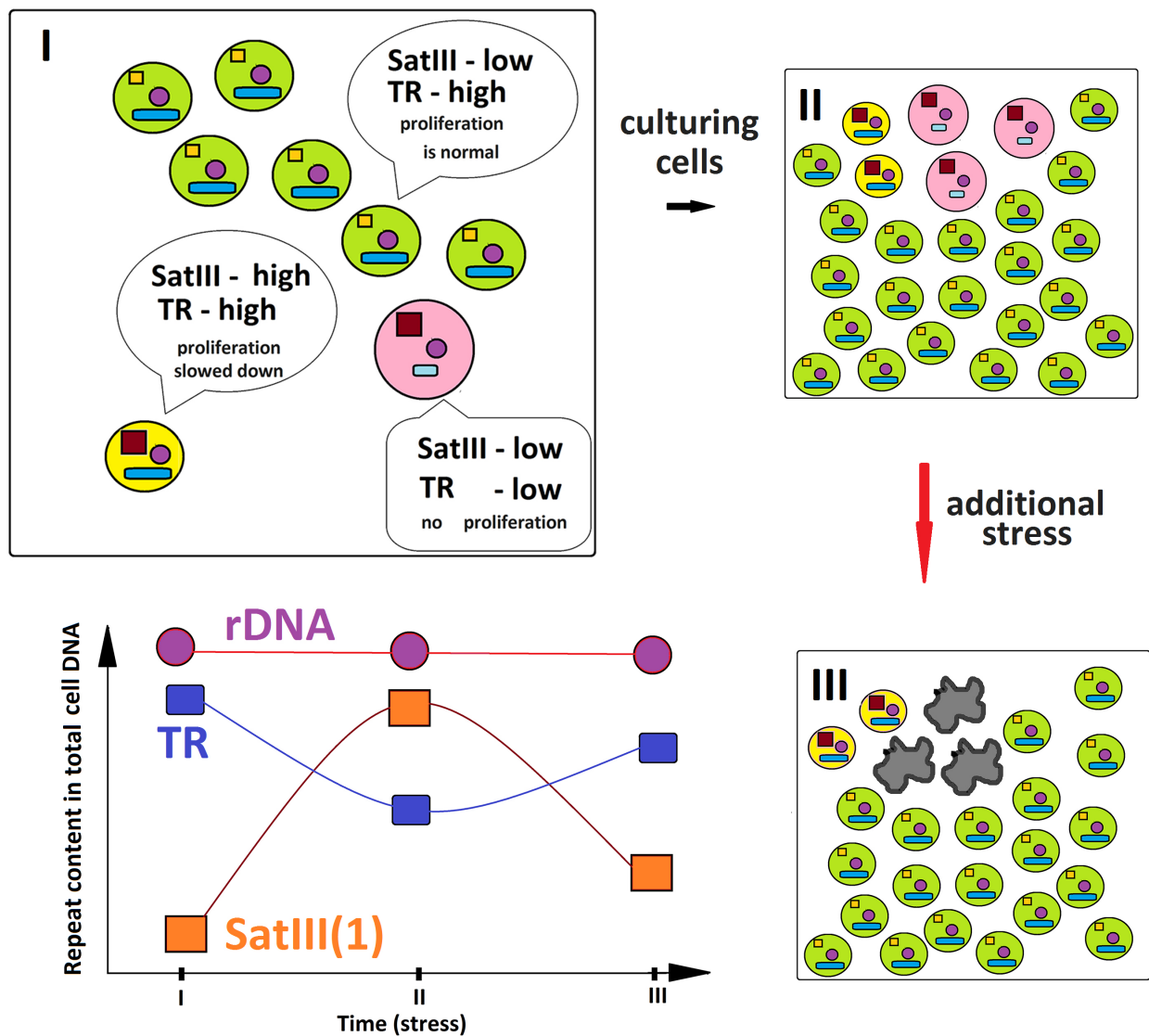


Fig. 7. A diagram illustrating SatIII (1) repeat copy number variation (CNV) in the pool of HSFs. See explanations in the text.

come the basis for a ‘pendulum’ model of SatIII (1) dynamics we proposed early [53] and corroborated in the present study.

The stress evokes an increase of RNASATIII (1) amount in HSFs during normal growth (Figs. 1,6). Transcription of the two fractions of satellite III, localized on chromosome 1 and chromosome 9, depends on the stress type. A high ROS level during cultivation induces an augmentation of RNASATIII (1) transcripts and a decrease of RNASATIII (9) transcripts. By contrast, a heat shock induces an augmentation of RNASATIII (9) amount and a decrease of RNASATIII (1) amount by several times (Fig. 6). As shown earlier, decondensation and transcription of heterochromatin during replicative senescence (when oxidative stress is increased) were observed for SatIII (1) fragment only, but not for SatIII (9) fragment [34].

The different patterns of stress response found in the two satellite III fragments seem to be associated with dif-

ferent mechanisms of transcription activation in these chromatin regions. For SatIII (9), a transcription inducer is heat shock factor [31–33]. A factor that triggers SatIII (1) transcription under oxidative stress and blocks transcription under heat shock is still unknown.

A bulk of data obtained in recent decades has shown that SatIII (1) repeat CNV in the same cell pool is a process typical for each type of cultivated and primary cells. The augmentation of SatIII (1) copy numbers after a stress impact of medium intensity and the decline after a stronger impact was earlier observed for cultivated human blood lymphocytes, mesenchymal stem cells, and skin fibroblasts [35,39]. Similar changes were observed in healthy human blood leucocytes under an affective stress [52]. On the peak of stress development, SatIII (1) copy number increased and TR copy number decreased in the leucocyte DNA. After the stress reverse changes were observed in the contents of the two types of DNA repeats. The same regularity was

observed in the cells from various human brain regions – a negative correlation between SatIII (1) and TR contents. A chronic stress favors elimination of the cells with high SatIII (1) content from blood *in vivo*. Perhaps that is why blood leucocyte DNA isolated from SZ patients contained low copy numbers of SatIII (1) [62].

We believe that the increase in SatIII (1) content in some cells of the pool is a manifestation of a general mechanism that is aimed at division arrest in cells with damaged chromatin. A high content of SatIII (1) in the cell is associated with blocking changes in the chromatin structure in response to proliferative and other stimuli. Such cells are subject to being eliminated from the pool; the more actively, the higher the stress in the body. At a relatively low level of stress, these cells accumulate in the pool during senescence. These cells are harmful ballast, as they can disrupt the functional activity of the entire cell population. This is especially true for cells of the nervous tissue that are involved in signal transmission along the cell chain.

It remains unknown what causes the arrest of chromatin mobility under stress conditions, and we do not consider the large size of SatIII (1) as the major cause of arrest. Other satellite chromatin fragments seem to be also involved in a similar scheme of CNVs. This mechanism warrants further research. First, answers to the following questions should be obtained.

(1) How does stress increase the size of the SatIII (1) repeat block in some cells of a normal (non-cancer) cell pool? The transcription from the satellite repeats is launched in most cells of the pool, but just a small fraction of the cells demonstrates an increased abundance of the repeat. One can assume that these cells may have an elevated level of reverse transcriptase, or their 1q12 region contains an increased number of chromatin break sites, where the hybrid molecules can be inserted.

(2) Are there any CNVs of other repeats, such as SatIII (9), during senescence and stress?

(3) What is the difference between the transcription activation mechanisms of the two fragments of satellite III, which are localized on chromosomes 1 and 9? Why is SatIII (1) transcription activation linked to SatIII (9) transcription suppression?

5. Conclusions

During human skin fibroblast cultivation, cells with increased SatIII (1q12) content accumulated in the cell pool under conditions of exaggerated oxidative stress intrinsic to schizophrenia. This fraction of cells decreased after the additional impact of exogenous stress. The process of SatIII increase/reduction seems to be oscillatory.

Availability of Data and Materials

The datasets used and/or analyzed during the current study are available from the corresponding author on reasonable request.

Author Contributions

ESE, NNV and VLI designed the study; ESE and LVK worked with cell cultures and performed DNA isolation and ROS assay; EAS determined the ribosomal repeat count and performed fluorescence microscopy; TAS determined the mtDNA and TR abundance; LNP and NNV wrote the text; LNP translated the text to English language; RVV and VLI statistically processed the data obtained; LNP, SIK and SVK made substantial contributions to data analysis and interpretation; SIK and SVK supervised the research. All authors contributed to editorial changes in the manuscript. All authors read and approved the final manuscript.

Ethics Approval and Consent to Participate

The study was carried out in accordance with the latest version of the Declaration of Helsinki and was approved by the Independent Interdisciplinary Ethics Committee on Ethical Review for Clinical Studies (Protocol No. 4 dated March 15, 2019 for the scientific minimally interventional study “Molecular and neurophysiological markers of endogenous human psychoses”). All participants provided written informed consent to participate in the study after the procedures had been completely explained.

Acknowledgment

Not applicable.

Funding

This research received funding within the frameworks of a State Assignment of the Ministry of Education and Science of the Russian Federation (#FGFF-2022-0007).

Conflict of Interest

The authors declare no conflict of interest.

References

- [1] Cooke HJ, Hindley J. Cloning of human satellite III DNA: different components are on different chromosomes. *Nucleic Acids Research*. 1979; 6: 3177–3197.
- [2] Higgins MJ, Wang HS, Shtromas I, Haliotis T, Roder JC, Holden JJ, *et al.* Organization of a repetitive human 1.8 kb KpnI sequence localized in the heterochromatin of chromosome 15. *Chromosoma*. 1985; 93: 77–86.
- [3] Moyzis RK, Albright KL, Bartholdi MF, Cram LS, Deaven LL, Hildebrand CE, *et al.* Human chromosome-specific repetitive DNA sequences: novel markers for genetic analysis. *Chromosoma*. 1987; 95: 375–386.
- [4] Choo KH, Earle E, Vissel B, Kalitsis P. A chromosome 14-specific human satellite III DNA subfamily that shows variable presence on different chromosomes 14. *American Journal of Human Genetics*. 1992; 50: 706–716.
- [5] Therkelsen AJ, Nielsen A, Kølvrå S. Localisation of the classical DNA satellites on human chromosomes as determined by primed in situ labelling (PRINS). *Human Genetics*. 1997; 100: 322–326.
- [6] Kretz M, Siprashvili Z, Chu C, Webster DE, Zehnder A, Qu K,

- et al.* Control of somatic tissue differentiation by the long non-coding RNA TINCR. *Nature*. 2013; 493: 231–235.
- [7] Lee JT, Bartolomei MS. X-inactivation, imprinting, and long noncoding RNAs in health and disease. *Cell*. 2013; 152: 1308–1323.
 - [8] Lv J, Cui W, Liu H, He H, Xiu Y, Guo J, *et al.* Identification and characterization of long non-coding RNAs related to mouse embryonic brain development from available transcriptomic data. *PLoS One*. 2013; 8: e71152.
 - [9] Johansson MM, Pottmeier P, Suciú P, Ahmad T, Zaghlool A, Halvardson J, *et al.* Novel Y-Chromosome Long Non-Coding RNAs Expressed in Human Male CNS During Early Development. *Frontiers in Genetics*. 2019; 10: 891.
 - [10] Sulayman A, Tian K, Huang X, Tian Y, Xu X, Fu X, *et al.* Genome-wide identification and characterization of long non-coding RNAs expressed during sheep fetal and postnatal hair follicle development. *Scientific Reports*. 2019; 9: 8501.
 - [11] Kuehner JN, Bruggeman EC, Wen Z, Yao B. Epigenetic Regulations in Neuropsychiatric Disorders. *Frontiers in Genetics*. 2019; 10: 268.
 - [12] Deng B, Cheng X, Li H, Qin J, Tian M, Jin G. Microarray expression profiling in the denervated hippocampus identifies long noncoding RNAs functionally involved in neurogenesis. *BMC Molecular Biology*. 2017; 18: 15.
 - [13] Aprea J, Lesche M, Massalini S, Prenninger S, Alexopoulou D, Dahl A, *et al.* Identification and expression patterns of novel long non-coding RNAs in neural progenitors of the developing mammalian cortex. *Neurogenesis (Austin, Tex.)*. 2015; 2: e995524.
 - [14] Jolly C, Metz A, Govin J, Vigneron M, Turner BM, Khochbin S, *et al.* Stress-induced transcription of satellite III repeats. *The Journal of Cell Biology*. 2004; 164: 25–33.
 - [15] Metz A, Soret J, Vourc'h C, Tazi J, Jolly C. A key role for stress-induced satellite III transcripts in the relocalization of splicing factors into nuclear stress granules. *Journal of Cell Science*. 2004; 117: 4551–4558.
 - [16] Eymery A, Souchier C, Vourc'h C, Jolly C. Heat shock factor 1 binds to and transcribes satellite II and III sequences at several pericentromeric regions in heat-shocked cells. *Experimental Cell Research*. 2010; 316: 1845–1855.
 - [17] Ugarković Đ, Sermek A, Ljubić S, Feliciello I. Satellite DNAs in Health and Disease. *Genes*. 2022; 13: 1154.
 - [18] Pezer Z, Brajković J, Feliciello I, Ugarković Đ. Satellite DNA-mediated effects on genome regulation. *Genome Dynamics*. 2012; 7: 153–169.
 - [19] Biscotti MA, Canapa A, Forconi M, Olmo E, Barucca M. Transcription of tandemly repetitive DNA: functional roles. *Chromosome Research: an International Journal on the Molecular, Supramolecular and Evolutionary Aspects of Chromosome Biology*. 2015; 23: 463–477.
 - [20] Thakur J, Packiaraj J, Henikoff S. Sequence, Chromatin and Evolution of Satellite DNA. *International Journal of Molecular Sciences*. 2021; 22: 4309.
 - [21] Louzada S, Lopes M, Ferreira D, Adegá F, Escudeiro A, Gama-Carvalho M, *et al.* Decoding the Role of Satellite DNA in Genome Architecture and Plasticity—An Evolutionary and Clinical Affair. *Genes*. 2020; 11: 72.
 - [22] Place RF, Noonan EJ. Non-coding RNAs turn up the heat: an emerging layer of novel regulators in the mammalian heat shock response. *Cell Stress & Chaperones*. 2014; 19: 159–172.
 - [23] Ugarković Đ. Functional elements residing within satellite DNAs. *EMBO Reports*. 2005; 6: 1035–1039.
 - [24] Chatterjee M, Sengupta S. Human satellite III long noncoding RNA imparts survival benefits to cancer cells. *Cell Biology International*. 2022; 46: 611–627.
 - [25] Goenka A, Sengupta S, Pandey R, Parihar R, Mohanta GC, Mukerji M, *et al.* Human satellite-III non-coding RNAs modulate heat-shock-induced transcriptional repression. *Journal of Cell Science*. 2016; 129: 3541–3552.
 - [26] Valgardsdóttir R, Chioldi I, Giordano M, Rossi A, Bazzini S, Ghigna C, *et al.* Transcription of Satellite III non-coding RNAs is a general stress response in human cells. *Nucleic Acids Research*. 2008; 36: 423–434.
 - [27] Giordano M, Infantino L, Biggiogera M, Montecucco A, Bi-amonti G. Heat Shock Affects Mitotic Segregation of Human Chromosomes Bound to Stress-Induced Satellite III RNAs. *International Journal of Molecular Sciences*. 2020; 21: 2812.
 - [28] Sengupta S, Parihar R, Ganesh S. Satellite III non-coding RNAs show distinct and stress-specific patterns of induction. *Biochemical and Biophysical Research Communications*. 2009; 382: 102–107.
 - [29] Feliciello I, Pezer Ž, Sermek A, Bruvo Mađarić B, Ljubić S, Ugarković Đ. Satellite DNA-Mediated Gene Expression Regulation: Physiological and Evolutionary Implication. *Progress in Molecular and Subcellular Biology*. 2021; 60: 145–167.
 - [30] Rizzi N, Denegri M, Chioldi I, Corioni M, Valgardsdóttir R, Cobianchi F, *et al.* Transcriptional activation of a constitutive heterochromatic domain of the human genome in response to heat shock. *Molecular Biology of the Cell*. 2004; 15: 543–551.
 - [31] Jolly C, Konecny L, Grady DL, Kutsikova YA, Cotto JJ, Morimoto RI, *et al.* In vivo binding of active heat shock transcription factor 1 to human chromosome 9 heterochromatin during stress. *The Journal of Cell Biology*. 2002; 156: 775–781.
 - [32] Vourc'h C, Dufour S, Timcheva K, Seigneurin-Berny D, Verdell A. HSF1-Activated Non-Coding Stress Response: Satellite lncRNAs and Beyond, an Emerging Story with a Complex Scenario. *Genes*. 2022; 13: 597.
 - [33] Morimoto M, Boerkoel CF. The role of nuclear bodies in gene expression and disease. *Biology*. 2013; 2: 976–1033.
 - [34] Erukashvily NI, Donev R, Waisertreiger ISR, Podgornaya OI. Human chromosome 1 satellite 3 DNA is decondensed, demethylated and transcribed in senescent cells and in A431 epithelial carcinoma cells. *Cytogenetic and Genome Research*. 2007; 118: 42–54.
 - [35] Konkova MS, Ershova ES, Savinova EA, Malinovskaya EM, Shmarina GV, Martynov AV, *et al.* 1Q12 Loci Movement in the Interphase Nucleus Under the Action of ROS Is an Important Component of the Mechanism That Determines Copy Number Variation of Satellite III (1q12) in Health and Schizophrenia. *Frontiers in Cell and Developmental Biology*. 2020; 8: 386.
 - [36] Ting DT, Lipson D, Paul S, Brannigan BW, Akhavanfard S, Coffman EJ, *et al.* Aberrant overexpression of satellite repeats in pancreatic and other epithelial cancers. *Science (New York, N.Y.)*. 2011; 331: 593–596.
 - [37] Eymery A, Horard B, El Atifi-Borel M, Fourel G, Berger F, Vitte AL, *et al.* A transcriptomic analysis of human centromeric and pericentric sequences in normal and tumor cells. *Nucleic Acids Research*. 2009; 37: 6340–6354.
 - [38] Bersani F, Lee E, Kharchenko PV, Xu AW, Liu M, Xega K, *et al.* Pericentromeric satellite repeat expansions through RNA-derived DNA intermediates in cancer. *Proceedings of the National Academy of Sciences of the United States of America*. 2015; 112: 15148–15153.
 - [39] Ershova ES, Malinovskaya EM, Konkova MS, Veiko RV, Umrjukhin PE, Martynov AV, *et al.* Copy Number Variation of Human Satellite III (1q12) With Aging. *Frontiers in Genetics*. 2019; 10: 704.
 - [40] Ershova ES, Malinovskaya EM, Golimbet VE, Lezheiko TV, Zakharova NV, Shmarina GV, *et al.* Copy number variations of satellite III (1q12) and ribosomal repeats in health and schizophrenia. *Schizophrenia Research*. 2020; 223: 199–212.
 - [41] Shigenaga MK, Ames BN. Assays for 8-hydroxy-2'-

- deoxyguanosine: a biomarker of in vivo oxidative DNA damage. *Free Radical Biology & Medicine*. 1991; 10: 211–216.
- [42] Pilger A, Rüdiger HW. 8-Hydroxy-2'-deoxyguanosine as a marker of oxidative DNA damage related to occupational and environmental exposures. *International Archives of Occupational and Environmental Health*. 2006; 80: 1–15.
- [43] Valdiglesias V, Giunta S, Fenech M, Neri M, Bonassi S. γ H2AX as a marker of DNA double strand breaks and genomic instability in human population studies. *Mutation Research*. 2013; 753: 24–40.
- [44] Guo S, Chen X. The human Nox4: gene, structure, physiological function and pathological significance. *Journal of Drug Targeting*. 2015; 23: 888–896.
- [45] Niwa JI, Yamada SI, Ishigaki S, Sone J, Takahashi M, Katsuno M, *et al.* Disulfide bond mediates aggregation, toxicity, and ubiquitylation of familial amyotrophic lateral sclerosis-linked mutant SOD1. *The Journal of Biological Chemistry*. 2007; 282: 28087–28095.
- [46] Bellezza I, Giambanco I, Minelli A, Donato R. Nrf2-Keap1 signaling in oxidative and reductive stress. *Biochimica et Biophysica Acta. Molecular Cell Research*. 2018; 1865: 721–733.
- [47] Ngo V, Duennwald ML. Nrf2 and Oxidative Stress: A General Overview of Mechanisms and Implications in Human Disease. *Antioxidants (Basel, Switzerland)*. 2022; 11: 2345.
- [48] Green DR. The Mitochondrial Pathway of Apoptosis Part II: The BCL-2 Protein Family. *Cold Spring Harbor Perspectives in Biology*. 2022; 14: a041046.
- [49] Green DR. The Mitochondrial Pathway of Apoptosis: Part I: MOMP and Beyond. *Cold Spring Harbor Perspectives in Biology*. 2022; 14: a041038.
- [50] Peña-Martínez C, Rickman AD, Heckmann BL. Beyond autophagy: LC3-associated phagocytosis and endocytosis. *Science Advances*. 2022; 8: eabn1702.
- [51] Chestkov IV, Jestkova EM, Ershova ES, Golimbet VE, Lezheiko TV, Kolesina NY, *et al.* Abundance of ribosomal RNA gene copies in the genomes of schizophrenia patients. *Schizophrenia Research*. 2018; 197: 305–314.
- [52] Umriukhin PE, Ershova ES, Filev AD, Agafonova ON, Martynov AV, Zakharova NV, *et al.* The Psychoemotional Stress-Induced Changes in the Abundance of SatIII (1q12) and Telomere Repeats, but Not Ribosomal DNA, in Human Leukocytes. *Genes*. 2022; 13: 343.
- [53] Porokhovnik LN, Veiko NN, Ershova ES, Kostyuk SV. The Role of Human Satellite III (1q12) Copy Number Variation in the Adaptive Response during Aging, Stress, and Pathology: A Pendulum Model. *Genes*. 2021; 12: 1524.
- [54] Ershova ES, Shmarina GV, Porokhovnik LN, Zakharova NV, Kostyuk GP, Umriukhin PE, *et al.* *In Vitro* Analysis of Biological Activity of Circulating Cell-Free DNA Isolated from Blood Plasma of Schizophrenic Patients and Healthy Controls. *Genes*. 2022; 13: 551.
- [55] Korsmeyer SJ, Shutter JR, Veis DJ, Merry DE, Oltvai ZN. Bcl-2/Bax: a rheostat that regulates an anti-oxidant pathway and cell death. *Seminars in Cancer Biology*. 1993; 4: 327–332.
- [56] Ermakov EA, Dmitrieva EM, Parshukova DA, Kazantseva DV, Vasilieva AR, Smirnova LP. Oxidative Stress-Related Mechanisms in Schizophrenia Pathogenesis and New Treatment Perspectives. *Oxidative Medicine and Cellular Longevity*. 2021; 2021: 8881770.
- [57] Ershova ES, Shmarina GV, Martynov AV, Zakharova NV, Veiko RV, Umriukhin PE, *et al.* NADPH-oxidase 4 gene overexpression in peripheral blood lymphocytes of the schizophrenia patients. *PLoS One*. 2022; 17: e0269130.
- [58] Seredenina T, Sorce S, Herrmann FR, Ma Mulone XJ, Plastre O, Aguzzi A, *et al.* Decreased NOX2 expression in the brain of patients with bipolar disorder: association with valproic acid prescription and substance abuse. *Translational Psychiatry*. 2017; 7: e1206.
- [59] Czarny P, Bialek K, Ziolkowska S, Strycharz J, Sliwinski T. DNA damage and repair in neuropsychiatric disorders. What do we know and what are the future perspectives? *Mutagenesis*. 2020; 35: 79–106.
- [60] Wu Y, Chen M, Jiang J. Mitochondrial dysfunction in neurodegenerative diseases and drug targets via apoptotic signaling. *Mitochondrion*. 2019; 49: 35–45.
- [61] Mahadik SP, Mukherjee S. Cultured skin fibroblasts as a cell model for investigating schizophrenia. *Journal of Psychiatric Research*. 1996; 30: 421–439.
- [62] Ershova ES, Agafonova ON, Zakharova NV, Bravve LV, Jestkova EM, Golimbet VE, *et al.* Copy Number Variation of Satellite III (1q12) in Patients With Schizophrenia. *Frontiers in Genetics*. 2019; 10: 1132.
- [63] Rupa DS, Hasegawa L, Eastmond DA. Detection of chromosomal breakage in the 1cen-1q12 region of interphase human lymphocytes using multicolor fluorescence in situ hybridization with tandem DNA probes. *Cancer Research*. 1995; 55: 640–645.
- [64] Surrallés J, Darroudi F, Natarajan AT. Low level of DNA repair in human chromosome 1 heterochromatin. *Genes, Chromosomes & Cancer*. 1997; 20: 173–184.
- [65] Zindel J, Kubes P. DAMPs, PAMPs, and LAMPs in Immunity and Sterile Inflammation. *Annual Review of Pathology*. 2020; 15: 493–518.
- [66] Ermakov AV, Konkova MS, Kostyuk SV, Izevskaya VL, Baranova A, Veiko NN. Oxidized extracellular DNA as a stress signal in human cells. *Oxidative Medicine and Cellular Longevity*. 2013; 2013: 649747.